NASA TECHNICAL NOTE

NASA TN D-6662

HIGH-CAPACITY, COMPACT VORTEX VALVE FOR INCREASING STABILITY OF SUPERSONIC MIXED-COMPRESSION INLETS

by Vernon D. Gebben

Lewis Research Center
Cleveland, Ohio 44135

NATIONAL AERONAUTICS AND SPACE ADMINISTRATION • WASHINGTON, D. C. • FEBRUARY 1972

1. Report No. NASA TN D-6662	2. Government Accession No.	3. Recipient's Catalog No.
4. Title and Subtitle HIGH-CAPACITY, COMPACT VORTEX VALVE FOR INCREASING STABILITY OF SUPERSONIC MIXED-COMPRESSION INLETS		5. Report Date February 1972 6. Performing Organization Code
7. Author(s) Vernon D. Gebben		8. Performing Organization Report No. E-6600 10. Work Unit No. 764-74
9. Performing Organization Name and Address Lewis Research Center National Aeronautics and Space Administration Cleveland, Ohio 44135		11. Contract or Grant No. 13. Type of Report and Period Covered Technical Note
12. Sponsoring Agency Name and Address National Aeronautics and Space Administration Washington, D.C. 20546		14. Sponsoring Agency Code

15. Supplementary Notes

16. Abstract

A special vortex valve was developed for increasing the stability margin of supersonic jet-engine inlets without the use of moving mechanical parts. A compact valve with high flow capacity and with high gain was obtained by using a unique outer wall in the vortex chamber instead of the usual cylindrical shape. This report describes the physical features of the valve, gives the steady pressure-flow characteristics measured on scaled models, and provides procedures for adjusting the operating pressure, flow capacity, and gain through systematic changes in geometry.

17. Key Words (Suggested by Author(s)) Engine inlets Intake systems Vortexes Valves Fluidics Automatic control valves	18. Distribution Statement Unclassified - unlimited	
19. Security Classif. (of this report) Unclassified	20. Security Classif. (of this page) Unclassified	21. No. of Pages 34
		22. Price* $3.00

* For sale by the National Technical Information Service, Springfield, Virginia 22151

HIGH-CAPACITY, COMPACT VORTEX VALVE FOR INCREASING STABILITY OF SUPERSONIC MIXED-COMPRESSION INLETS

by Vernon D. Gebben

Lewis Research Center

SUMMARY

The stability margin of supersonic jet-engine inlets operating at high performance levels can be increased by controlling bypass flow drawn from the inlet throat region. A special vortex valve was developed as a possible means for controlling this flow without the use of moving mechanical parts.

This new valve has high flow capacity with desirable high gain characteristics. The ratio of maximum to minimum valve flow measured for the operating pressures expected in a Mach-2.5 inlet was 10 for this design. High gain was achieved by using a unique outer wall in the vortex chamber instead of the usual cylindrical shape. The result is a compact valve whose chamber diameter is 4 times the outlet diameter.

The report describes the physical features of the valve, gives design procedures, and gives the steady pressure-flow characteristics measured on one-sixth-scale models. To represent the valve performance, a new set of nondimensional variables were defined. An experimental study concluded that the desired operating pressures, flow capacity, and gain for jet-engine inlets can be obtained through systematic changes in valve geometry.

INTRODUCTION

The prototype vortex valve described in this report was designed especially for use in a throat bleed system of an experimental Mach-2.5 inlet. The purpose of the valve is to extend the stability range of a mixed-compression inlet by enabling it to self-regulate the throat bleed.

Mixed-compression inlets provide an efficient process for supplying air to jet engines during supersonic flight. Maximum performance for this type of inlet results when the normal shock is located close to the throat. The shock can be accurately

positioned with the bypass doors illustrated in figure 1. For example, when the shock moves upstream from the desired location, the servosystem increases the open area of the bypass doors. Flow then increases through the doors and the normal shock returns to its proper position.

Inlet unstarts, however, can occur when pressure disturbances move the shock too fast for the servosystem. The servosystem is then unable to prevent the shock from becoming expelled from the inlet. During unstart, the jet engine experiences a large decrease in thrust and possibly a flameout. If the unstart pulsates, the entire propulsion system receives severe vibrations.

Throat bleed systems are used to stabilize inlets while maintaining an efficient inlet diffusion process. These systems generally attempt to maintain a near-constant pressure in the throat. This action restrains a shock from moving upstream of the throat and thereby makes the inlet less sensitive to engine load changes and atmospheric disturbances during flight.

The effectiveness of inlet throat bleed systems was reported by Sanders and Mitchell (ref. 1). They obtained large stability margins against unstarts by controlling throat bleeds with variable choked exits, self-acting mechanical valves, and vortex valves.

The technique of using vortex valves to increase the stability margin of mixed-compression inlets was reported by Moorehead (ref. 2). Vortex valves provide advantages of high reliability and fast response, since they contain no moving mechanical parts. Their quiescent flow consumption and relatively large size, however, present disadvantages in this application. To minimize these disadvantages, a special vortex valve was designed.

This report describes the physical features and performance of the valve developed for the project reported in reference 1. The development program used models that were one-sixth the size of the valves later used in the experimental inlet tested in the 10- by 10-Foot Supersonic Wind Tunnel at Lewis.

Experiments on the models revealed that small changes in geometry greatly affect the pressure-flow characteristics. These effects and the best design determined for the given inlet are described in the report. The report also covers test conditions and considerations of dynamic flow similarity for one-sixth-scale models.

DESCRIPTION OF THE VALVE DESIGN

A design configuration often used to describe a typical vortex valve and its operating principles is shown in figure 2. The valve consists of a short cylindrical chamber enclosed by end walls, two inlets, and an outlet. The radial passageway allows the fluid to enter the chamber and flow to the outlet orifice without appreciable pressure drop. The tangential nozzle injects fluid tangentially along the cylindrical wall and generates

a vortex flow pattern in the chamber. The fluid leaves the chamber through the orifice located at the center of one of the end walls.

The valve acts as a variable restrictor controlled by the confined vortex. For example, an increase in tangential nozzle flow increases the circulation (vortex strength) which reduces the pressure near the chamber center. This reduction in pressure immediately upstream of the outlet orifice reduces the outlet flow.

Maximum flow restriction occurs when the tangential flow and outlet flow are equal. Then the flow through the radial passageway is zero. This special operating condition is referred to as the "cutoff" condition.

In the jet-engine application shown in figure 3, the tangential nozzle pressure P_t could be obtained far downstream of the normal shock, near the compressor, where the pressure is essentially independent of shock position (symbols are defined in appendix C). Pressure P_t then serves as a reference pressure. The radial supply pressure P_r obtained from the inlet throat is the variable that controls the bypass flow.

When the shock is in its proper location, P_r is relatively low with respect to P_t. This pressure difference produces a strong vortex field within the valve. If designed correctly, the valve would then operate at cutoff to completely stop flow through the throat bypass bleed entrance.

As the normal shock moves upstream, pressure P_r increases. The result is a decrease in vortex strength that permits an increase in bypass bleed. The bypass reaches its maximum flow when the shock is upstream of the bleed entrance. Pressure P_r then produces a weak vortex field that offers minimum resistance through the vortex chamber.

This system can provide much larger increases in bypass flow with forward shock movement than a conventional fixed-exit bleed system. And just as important, the quiescent flow consumption during normal operation can be limited to the same amount as provided by the conventional choked-exit bleed.

The design goal is to have the maximum throttling range for the available operating pressures. This requires high gain near cutoff. The throttling range for comparing different valve designs can be expressed as the ratio of maximum to minimum flow through the valve. For the jet-engine inlet application, this ratio will be called "vortex bypass ratio."

Vortex bypass ratio is defined herein as the ratio of maximum to minimum mass flow through the valve for a specified pressure range when the valve is operated with a constant tangential supply pressure P_t. This term was adopted to prevent confusion with "turndown ratio" which the literature generally defines as the ratio of nonswirl flow (maximum flow) to the cutoff (minimum flow) when the valve is operated with a constant radial supply pressure P_r.

The vortex bypass ratio obtained with the special valve described in this report was 10. This ratio is appreciably higher than that obtained with a more conventional valve of equivalent size. Figure 4 shows the steady pressure-flow characteristics of the two valves. The normalized coordinates will be explained in another section. Figure 4 illustrates that a higher vortex bypass ratio was obtained by having high gain (steep slope) in the specified jet-engine inlet operating range which occurs near the cutoff condition. This high gain characteristic was produced by a special valve shape.

The new valve shown in figures 5 and 6 has several distinctive physical features. For example, the ratio of chamber diameter to outlet orifice diameter is approximately 4, which is half the diameter ratio of most high-gain, high-flow-capacity, vortex valves. The outer wall is different from the usual cylindrical shape. The valve has two radial passageways that are slightly offset from the true radial. The single tangential nozzle is composed of a row of holes between the end walls instead of a conventional rectangular slot. The valve has two outlet orifices. This configuration was developed from the following viewpoints and considerations.

The ratio of chamber diameter to outlet diameter that would provide minimum cutoff flow was experimentally investigated. Tests were conducted on vortex chambers that were similar to the valve illustrated in figure 2, except they had no radial inlets. The pressure at the chamber periphery was used to represent P_r for the cutoff condition in a vortex valve. The test units had identical tangential nozzles, identical outlet-orifice diameters, but different chamber diameters. Figure 7 shows the results of these tests. The vortex flow was unaffected by diameter ratio. This observation is supported analytically by Bauer (ref. 3).

However, it was concluded from other investigations that the throttling range of vortex valves is small for the diameter ratio of 2.5. There is not enough room for a radial inlet passageway that is large enough to offer negligible flow resistance during the nonswirl operation. Also, cutoff flow is greatly increased by radial inlets if the inlets occupy a large portion of the peripheral area of the chamber. Reduced performance probably results from increased turbulence, which causes an increase in the inflow through the boundary layers along the end walls.

The effect of radial-inlet size on the cutoff flow was reported by Greber, Koerper, and Taft (ref. 4). Their data displaying this effect were obtained from a variable-geometry valve that contained an annular slot in the end wall for the radial inlet and had two outlet orifices. Their final design, optimized for maximum turndown ratio, has a diameter ratio of 3.3 and a radial-inlet-slot width equal to 4.5 percent of the chamber diameter. According to their analysis, a larger radial inlet would decrease the turndown ratio.

In developing the valve for stabilizing the jet-engine inlet, it was concluded from reports and other experimental observations that a diameter ratio of 4 would be a reasonable size.

The outer wall of the new valve has an unusual, curved shape. To minimize the turbulence that degrades the cutoff flow, the outer wall is perpendicular to the radial passageway and is offset to permit the tangential flow to spread without impinging against the wall of the radial passageway. This offset is shown in figure 5, where it is designated by Y. The shape of the outer wall provides the high gain near the cutoff condition. High gain near cutoff seems to be caused by flow attaching to the outer wall between points a and b and between c and d in figure 5. This attachment is similar to the wall-attachment effect of fluid-jet amplifiers.

The purpose for two opposing radial inlets was to reduce or minimize turbulence by reducing the open space across the radial inlet and by providing symmetric radial inlet flow. The radial passageways are slightly offset from the true radial to provide the outer-wall offset Y while maintaining a shape to the outer wall that is nearly cylindrical. This radial-inlet offset (X in fig. 5) creates a counterswirl when the tangential nozzle flow is zero and changes the pressure-flow characteristics at the no swirl condition. This effect, however, is outside the operating range for the jet-engine application and, therefore, presents no problem.

The tangential nozzle developed for the valve consists of a row of holes instead of the rectangular slot. Tests with the rectangular slot displayed a problem due to leakage between the end plates and valve body at the thin web that separates the nozzle from the vortex chamber. To eliminate the problem, the sealing area was increased by using a row of drilled holes as shown in figure 5. A single drilled hole for the nozzle was considered but not used because the tangential flow across the chamber would be less uniform and would probably increase the mixing losses.

Two outlets are commonly used in applications where maximum turndown ratio is needed. The increase in turndown ratio results from the characteristic that the mass flow during the nonswirl condition doubles when two orifices are used instead of one. The cutoff flow rate, however, remains essentially unchanged. Hence, the ratio of maximum to minimum mass flow for two outlets is twice the ratio obtained for one outlet.

Evaluation tests were performed on a one-sixth-scale model of the unit tested experimentally in a mixed-compression inlet. Experiments were conducted to determine the effects of pressure and geometry changes. The results of these tests are presented in other sections of this report.

VALVE CONFIGURATION AND TEST CONDITIONS

Sixteen full-size valves operated in parallel were used to evaluate the effectiveness of vortex valves for stabilizing supersonic, mixed-compression inlets (ref. 1). The valve was designed for operating with a tangential supply pressure P_t of 8 N/cm^2 and

an exhaust pressure P_e of 1.0 N/cm^2. The radial supply pressure P_r was expected to be 3.5 N/cm^2 at cutoff and 5.6 N/cm^2 at the maximum flow condition. The valve had a 1.91-centimeter outlet diameter. This size was too large and the pressures were too low for convenient testing with existing equipment in our fluidics laboratory. A one-sixth-scale model operated at higher pressures was used to simulate the full-size unit.

Conditions for dynamic flow similarity of confined vortex flows were presented by Roschke and Pivirotto (ref. 5). Similarity requires equal tangential Mach number at the edge of the free stream near the outer wall, equal Reynolds number, equal Prandtl number, and similar geometry. Similar geometry requires exact scaling of both the geometry and the wall texture; otherwise, the boundary-layer flows, which markedly affect the valve performance, will be different. Changes in Mach number and Reynolds number appear unimportant for this application, where the ratio P_t/P_e equals 8 and the flow is turbulent. The Prandtl number requirement for modeling is essentially satisfied by using the same gas. Thus, modeling the vortex valve appears to present no basic problems.

Evaluation tests on models one-sixth full size were performed with room-temperature air (300 K). The outlet orifice was vented to the atmosphere. The tangential supply pressure P_t was 4 times the barometric pressure. A servosystem regulated P_t within 0.07 N/cm^2 of the set point. The radial supply pressure P_r was the control variable in these tests.

The test pressures resulted in a Reynolds number nearly identical to the Reynolds number for the full-scale unit operated under the design conditions. Appendix A derives the Reynolds number relation. Appendix B shows that the pressure ratio P_t/P_e of 4

TABLE I. - PRINCIPAL DIMENSIONS OF ONE-SIXTH-SCALE VALVES

Valve model	Total tangential nozzle area, A_t, mm^2	Number of tangential nozzles	Outer wall offset,[a] Y, mm	Total outlet orifice area, A_o, mm^2	Chamber depth, mm
A	0.63	2	0.51	15.7	6.50
B	.98	6			6.48
C	1.58	5			6.50
D	2.16	5			5.87
E	.98	6	.10		6.63
F	.98	6	.91		6.38
G	1.58	5	.51	24.8	6.50
H	1.58	5	.51	35.6	6.50
Recommended design	.83	6	.51	15.7	6.50

[a]See fig. 5.

instead of the required 8 has negligible effect on the pressure-flow characteristics of the valve in the operating range of interest, where the tangential nozzle flow is choked.

Figure 8 is a photograph of one of the test models. The model was constructed from acrylic sheet stock. The smooth, flat surfaces of the acrylic sheets were used to model the end-wall surfaces of the full-scale chamber.

Eight configurations were evaluated. Their basic geometries are listed in table I. Models A, B, C, and D were used to study performance changes caused by varying the total flow area of the tangential nozzles. Models E and F had different shapes for the chamber outer wall. Models G and H had different outlet-orifice diameters. The following section gives the results of the experimental investigation.

GEOMETRY EFFECTS

A small change in configuration can greatly affect the pressure-flow characteristics of vortex valves. To determine the best design for use in a jet-engine inlet, various tangential nozzles, outlet orifices, and chamber geometries were examined. The following data and observations should aid in making future modifications in the full-size vortex valve.

The steady pressure-flow characteristics presented in this report are described by two special nondimensional variables. The pressure variable is defined as

$$P_* = \frac{P_r - P_e}{P_t - P_e} \tag{1}$$

The flow variable is defined by

$$\dot{m}_* = \frac{\dot{m}_o}{\dot{m}_n} \tag{2}$$

where $\dot{m}_o$ is the outlet mass flow and $\dot{m}_n$ is the normalizing term determined by the outlet orifice size, gas temperature, and pressures at the cutoff point. Formulas and further details on $\dot{m}_n$ are given in appendix B. This appendix also contains data showing that a single curve of P_* as a function of $\dot{m}_*$ accurately represents the performance over a wide range of supply and exhaust pressures.

Four different sets of tangential nozzles in the basic chamber configuration of figure 6 were tested. The performance curves from these tests are shown in figure 9.

The upper ends of the curves terminate where the tangential inlet flow is zero. The lower ends of the curves, our main region of interest, terminate at the valve cutoff point, where the radial inlet flow is zero. Reduction in tangential nozzle area reduces the cutoff flow and reduces the cutoff pressure.

The performance of model C was expected to be midway between the performances of models B and D, since the tangential nozzle area of C is midway between those of B and D. However, the performance curve for model C is located close to the curve for model D. Also, the S-shape of the lower end of curve C could produce a jump action in the control system, thereby making the design unusable. The reasons for the S-shape of curve C and its shift toward curve D are unknown.

The cutoff points for models A, B, C, and D are plotted in figure 10. The line connecting the data points was used to evaluate the vortex field at cutoff for geometry changes. Cutoff points below the curve indicate a more effective vortex field, since less normalized flow is required.

Small geometrical changes in the outer wall had large effects near the cutoff point. Figure 11 shows the pressure-flow characteristics of model B, which was used as the reference model, and shows the characteristics of models E and F, which had changes in the outer-wall offset (dimension Y of fig. 5).

Dimension Y in model E was shortened from that of model B by 0.41 millimeter. This change raised the gain to the extent that the slope of the pressure-flow curve changed polarity, and the curve became S-shaped. This shape makes model E unusable for most control applications.

Dimension Y in model F was 0.41 millimeter longer than in model B. This change greatly reduced the gain near the cutoff point and made this model less desirable for the engine air inlet bypass applications. The performance of model F was very linear over the entire flow range. This characteristic is quite unique, since vortex valves are generally very nonlinear, with S-shaped curves. In figure 12, the cutoff point for model F is well above the reference line from figure 10. Therefore, the improvement in linearity was obtained at higher flows (lower efficiency) at the cutoff point.

The cutoff points for models B, E, and F in figure 12 are at slightly different flow values. The variation was probably due to variation in tangential nozzle size resulting from machining tolerances rather than being related to dimension Y.

The effect of changes in outlet orifice size is presented in figure 13. The changes were made by enlarging the outlet orifices of model C to produce models G and H. Other dimensions were unchanged. The larger outlet orifices increased the flow beyond the capability of the test bench. Consequently, the upper ends of the curves for models G and H in figure 13 terminated before the condition of zero tangential flow was reached.

Figure 13 shows that increasing the outlet area reduces $\dot{m}_*$ in the region near $P_* = 1$, where the swirl in the chamber is minimal. This effect can be explained by

considering the vortex valve as three flow resistors connected in series - these are radial inlet, chamber, and outlet resistance. When the size of the entire valve is changed, all resistors change proportionately. The result is a proportionate change in flow rate that has no effect on $\dot{m}_*$, since the normalizing term $\dot{m}_n$ in equation (2) is proportional to the outlet-orifice area. However, in models G and H, the outlet resistance was reduced by increasing the outlet-orifice diameter, while the radial and chamber resistances remained unchanged. Consequently, the flow ($\dot{m}_o$) through these valves was smaller than would have been obtained if the inlet and chamber had also been enlarged. This reduction in $\dot{m}_o$ reduces the value of $\dot{m}_*$ in equation (2).

Figure 14 compares the cutoff points for models C, G, and H with the reference line from figure 10. The cutoff points for enlarged outlets are below the reference line, indicating that they increased the effectiveness of the vortex field. The improvement, although small, is interesting to note, since the ratio of chamber diameter to outlet diameter had been reduced from 4 in model C to 2.7 in model H. However, as mentioned before, the flow capability away from the cutoff points was greatly reduced, thereby making the overall performance of models G and H inferior to the basic design performance of models A, B, C, and D. Unfortunately, an increase in flow capacity should, therefore, be accomplished by enlarging the entire valve rather than by changing the outlet orifice only.

The results from these tests on configuration changes give guidelines for changing the cutoff pressure, flow capacity, and gain. The following recommended methods were drawn from the tests:

(1) Increase cutoff pressure by increasing the tangential nozzle size.

(2) Increase gain by reducing the outer-wall offset (dimension Y in fig. 5).

(3) Increase flow capacity by proportionately increasing the size of the entire valve.

RECOMMENDED VALVE DESIGN FOR INITIAL TESTS ON MACH-2.5 INLET

A vortex valve design was selected for the operating pressure range estimated for the Mach-2.5, experimental, mixed-compression inlet. With the shock in its proper position, as shown in figure 3, the normalized pressure P_* will be approximately 0.35. When the shock moves upstream of the radial supply port, P_* will increase to approximately 0.65.

The predicted performance curve for the recommended valve design is shown in figure 15. Since this curve was obtained from proportional interpolation between the curves of models A and B, it is assumed to be an accurate representation. The maximum $\dot{m}_*$ for the given operating range is 0.47, the minimum is 0.046. Thus, a vortex bypass ratio of 10:1 seemed possible for the throat bleed system experiments described

in reference 1. The dimensions of the recommended valve design are given in table I (p. 6).

Pressure-flow measurements were made on one of the full-size valves before it was installed in the inlet. The valve had tangential nozzles that were 15 percent smaller than the nozzles corresponding to the recommended design in table I. Smaller nozzles could be used, since the throat bleed system was tested with a technique that used a higher pressure supplied to the tangential nozzles from an external source instead of pressure supplied from a source near the engine compressor, as originally planned.

The steady pressure-flow characteristics of the full-size valve are given in figure 16. As shown by the predicted performance curve, the gain of the full-size valve was lower than expected from the one-sixth-scale models. The full-size valve had characteristics almost identical to those shown in figure 11 for model F, which resulted from too large an offset of the outer wall (dimension Y in fig. 5). Offset Y in the full-size valve was the recommended value; that is, it was equivalent to the offsets used in models A, B, C, D, G, and H. Therefore, one would expect that the gain could be increased to the desired gain by reducing dimension Y. This modification has not been tried in the full-size vortex valve.

SUMMARY OF RESULTS

The project goal was to develop a vortex valve that has high gain in the operating range where the outlet flow is near minimum. This was achieved by using a unique configuration.

The ability to change the gain by altering the shape of the vortex chamber was a principal feature. Adjustable gain permitted the development of a compact valve whose chamber diameter is 4 times the outlet orifice diameter.

The effects of changes in tangential nozzle size, outlet orifice size, and chamber shape were examined on one-sixth-scale models of the valve designed for use in an experimental, Mach-2.5 inlet. The study showed that the desired operating pressures, flow capacity, and gain for the jet-engine inlet can be obtained through systematic changes in the valve configuration.

Lewis Research Center,
National Aeronautics and Space Administration,
Cleveland, Ohio, November 1, 1971,
764-74.

APPENDIX A

REYNOLDS NUMBER FOR VORTEX VALVE MODELING

The Reynolds number for modeling the vortex valve is derived from the standard equation

$$R_N = \frac{\rho V D}{\mu}$$

The Reynolds number R_N is determined for the valve operating at the cutoff condition. Furthermore, R_N is specified at the location in the vortex chamber where the flow is sonic. Hence, by definition, ρ is the fluid density where the flow is Mach 1, V is the velocity at Mach 1, D is the diameter where the flow is Mach 1, and μ is the dynamic viscosity where the flow is Mach 1.

From basic equations of ideal compressible fluid flow, we have V proportional to $\sqrt{T_t}$, ρ proportional to P_t/T_t, and μ approximately proportional to $\sqrt{T_t}$. The symbols T_t and P_t represent the upstream temperature and pressure of the tangential nozzles. Applying these relations to the R_N for two geometrically similar valves results in

$$\frac{R_{N,1}}{R_{N,2}} \approx \frac{D_1}{D_2} \frac{P_{t,1}}{P_{t,2}} \frac{T_{t,2}}{T_{t,1}}$$

The estimated values of P_t and T_t for the full-scale unit are 8.0 N/cm^2 and 367 K, respectively. The one-sixth-scale model evaluated in this report was tested with P_t = 40 N/cm^2 and T_t = 300 K. Thus, the R_N ratio is

$$\frac{R_{N,1}}{R_{N,2}} \approx 6\left(\frac{8.0}{40}\right)\left(\frac{300}{367}\right) \approx 1$$

Therefore, the R_N of the model approximates the R_N of the full-scale unit.

APPENDIX B

NONDIMENSIONAL VARIABLES FOR STEADY PRESSURE-FLOW CHARACTERISTICS

Various nondimensional graphs are used to predict the performance of vortex valves over their entire operating range when run at different pressures (refs. 6 to 8). A different set of normalized quantities was found more suited to the jet-engine inlet bypass application. In this appendix, these quantities are defined and data are provided to show that this representation is valid for the valve described in this report.

General Definitions

The steady pressure-flow characteristics of the vortex valve are represented by two special nondimensional variables. The pressure variable is defined by the equation

$$P_* = \frac{P_r - P_e}{P_t - P_e} \tag{B1}$$

where P_r is the radial supply pressure, P_e is the exhaust pressure, and P_t is the tangential nozzle supply pressure. The flow variable is defined by the equation

$$\dot{m}_* = \frac{\dot{m}_o}{\dot{m}_n} \tag{B2}$$

where $\dot{m}_o$ is the outlet mass flow, and $\dot{m}_n$ is a normalizing term.

This normalizing term is defined by the equation

$$\dot{m}_n = \dot{m}_i \left(\frac{A_o}{A_t}\right) \tag{B3}$$

where $\dot{m}_i$ is the theoretical (ideal) flow through the tangential nozzles, and A_o/A_t is the ratio of outlet orifice area to tangential nozzle area. Equation (B2) then takes the form

$$\dot{m}_* = \left(\frac{\dot{m}_o}{\dot{m}_i}\right)\left(\frac{A_t}{A_o}\right) \tag{B4}$$

The purpose of A_t/A_o is to equalize $\dot{m}_*$ for valves that have the same cutoff pressure but different-size orifices. At present, this area-ratio coefficient is the author's empirical term that seemed to work well in the design of the jet-engine inlet vortex valve. The purpose of $\dot{m}_i$ is to normalize the outlet flow $\dot{m}_o$ with respect to the theoretical maximum flow that can occur at the cutoff point. At the cutoff point, the ratio $\dot{m}_o/\dot{m}_i$ becomes the discharge coefficient C_{Dt} of the tangential nozzles, so that

$$\dot{m}_{*t} = C_{Dt}\left(\frac{A_t}{A_o}\right) \tag{B5}$$

Consequently, the normalized cutoff flow $\dot{m}_{*t}$ is unaffected by energy losses in the vortex chamber and in the outlet orifices. Those losses are reflected in the normalized cutoff pressure P_{*t} which is determined by equation (B1). For example, if energy losses are increased by surface roughness in the vortex chamber, the circulation will be reduced. The weaker vortex will have a smaller pressure drop across its field. The result will be a reduction in P_{*t}.

Determination of Normalizing Term for Choked Cutoff

The equation for computing the normalizing term $\dot{m}_n$ for use in equation (B2) depends on whether the tangential nozzle flow is choked or unchoked at the particular cutoff point obtained by reducing P_r while maintaining P_t and P_e constant. At cutoff, the flow and pressure drop through the radial inlet is zero. For this condition, the pressure drop across the tangential nozzles equals P_t minus P_{rt}, where P_{rt} is the radial supply pressure at the cutoff point. Thus, the flow through the tangential nozzles is considered choked when

$$\frac{P_{rt}}{P_t} \le \left(\frac{2}{k+1}\right)^{k/(k-1)} \tag{B6}$$

where k is the ratio of specific heats (eq. 4.15b and sect. 4.6 in ref. 9).

For the choked condition, the theoretical flow through the tangential nozzles can be expressed by the following equation (sect. 4.4 in ref. 9):

$$\dot{m}_i = \frac{CA_tP_t}{\sqrt{T_t}} \tag{B7}$$

where T_t is the gas temperature upstream of the tangential nozzles, and C is a constant. For air,

$$C = 0.0405 \qquad (kg)(\sqrt{K})/(N)(sec) \tag{B8}$$

The equation for $\dot{m}_n$ then becomes

$$\dot{m}_n = \frac{CA_oP_t}{\sqrt{T_t}} \tag{B9}$$

The tangential nozzle area is, therefore, not required in computing $\dot{m}_n$. This eliminates the problem that results when A_t is unknown or cannot be accurately measured.

The maximum flow that can pass through the "ideal" vortex valve occurs at $P_* = 1$. The ideal valve under this condition has no swirl in the chamber and no pressure drops between the radial supply and the outlet. Since $P_t = P_r$, the upstream pressure to the outlet orifices equals P_t. The equation for choked flow in the outlet orifices then can be written as

$$\dot{m}_o = \frac{CA_oP_t}{\sqrt{T_t}} \qquad \text{at } P_* = 1 \tag{B10}$$

Substituting equations (B9) and (B10) in equation (B2) yields

$$\dot{m}_* = 1 \qquad \text{at } P_* = 1 \tag{B11}$$

Thus, $\dot{m}_*$ can be considered as a flow variable that is normalized to the upper limit occurring at $P_* = 1$. This simplified relation is valid only for the case where the tangential nozzles are choked at the cutoff point.

Determination of Normalizing Term for Unchoked Cutoff

Isentropic flow through the tangential nozzles can be expressed by the following equation (sect. 4.4 in ref. 9):

$$\dot{m}_i = \frac{CA_t P_t \left(\frac{A^*}{A}\right)}{\sqrt{T_t}} \tag{B12}$$

where A^*/A is the conventional area-ratio function for one-dimensional compressible flow for the isentropic process. The equation for $\dot{m}_n$ then becomes

$$\dot{m}_n = \frac{CA_o P_t \left(\frac{A^*}{A}\right)}{\sqrt{T_t}} \tag{B13}$$

The value for A^*/A can be obtained directly from gas tables or calculated from the following equation:

$$\frac{A^*}{A} = \sqrt{\frac{2}{k-1}\left(\frac{k+1}{2}\right)^{(k+1)/(k-1)}\left[\left(\frac{P_{rt}}{P_t}\right)^{2/k} - \left(\frac{P_{rt}}{P_t}\right)^{(k+1)/k}\right]} \tag{B14}$$

The pressure P_{rt} is a function of P_t and P_e. It can easily be obtained by measuring the radial inlet pressure while the radial supply line is shut off with a mechanical valve. It can also be obtained from measurements recorded when variables P_* and $\dot{m}_*$ are plotted directly on an X-Y recorder during a test run.

Direct Recording of Normalized Pressure as Function of Normalized Outlet Mass Flow

The normalized variables can be recorded conveniently with an X-Y plotter during a test run if T_t, P_t, and P_e are maintained at constant values. It will be shown that the plot of P_* as a function of $\dot{m}_*$ is identical to a plot of P_r as a function of $\dot{m}_o$, except the coordinates and scaling have been changed.

To record the normalized pressure P_*, equation (B1) is rearranged in the following form:

$$P_* = \frac{P_r}{P_t - P_e} - \frac{P_e}{P_t - P_e} \tag{B15}$$

When P_t and P_e are constant, equation (B15) can be written as

$$P_* = \frac{P_r}{K_1} - K_2 \tag{B16}$$

where K_1 and K_2 are constants. Thus, P_* is directly related to P_r. By shifting the recorder's zero axis to the $-K_2$ position, P_* can be recorded directly by measuring a proportional amount of P_r.

The normalized outlet mass flow $\dot{m}_*$ can be recorded directly from $\dot{m}_o$ measurements if $\dot{m}_*$ and $\dot{m}_o$ are proportional to each other. According to equation (B2), this relation exists when $\dot{m}_n$ is constant. Equations (B9) and (B13) show that $\dot{m}_n$ is constant when T_t, P_t, and P_e are constant. Therefore, $\dot{m}_*$ can be recorded directly by measuring a proportional amount of $\dot{m}_o$ while maintaining T_t, P_t, and P_e constant.

Experimental Verification of Normalizing Technique

Normalized representations in general seem limited by vortex-valve characteristics that change with changes in operating pressures. Unpredictable performance results from compressible and viscous effects that influence the amount of inflow along the end walls, unknown mixing efficiency of the tangential and radial inlet flows, secondary vortices in the chamber, turbulence, and velocity limits. The effective range of a normalization must be experimentally determined for each valve design. The following data show that the normalized curve for each model evaluated in this report is moderately insensitive to changes in P_t, P_r, and P_e. The curve is sufficiently accurate to represent the performance of the valve over the expected operating conditions of the engine inlet.

Figure 17 shows a valve operating with a variable P_r at three values of P_t and at constant P_e. The three curves could be averaged to form a single curve that would represent the valve for any P_t in the pressure range tested. Similar conclusions are drawn from figures 18 and 19, which represent two other valve designs. Thus, the normalized curve accounts for changes in P_r and P_t.

Figure 20 shows data obtained with a variable P_r at five values of P_e and at constant P_t. In this figure, the pressure scale has been expanded to separate the data points. These points are reasonably close to a single curve that could represent the valve over a wide range of P_r and P_e.

Data obtained with variable P_e, four values of P_r, and constant P_t are shown in figure 21. Again, the points are close to a single curve that could represent the effects of changes in P_r and P_e.

It was concluded from these experiments that a plot of P_* as a function of $\dot{m}_*$ accurately represents valve performance over a wide range of supply and exhaust pressures. The data show that the nondimensional characteristics are quite independent of

Mach number when the pressure ratio P_t/P_e exceeds 3. Therefore, the normalized curve can be used to accurately predict the performance for any jet-engine inlet operating condition.

APPENDIX C

SYMBOLS

A_o total outlet orifice area, mm^2

A_t total tangential nozzle area, mm^2

A^*/A conventional area-ratio function for one-dimensional compressible flow, dimensionless

C constant (eq. (B8)), $(kg)(\sqrt{K})/(N)(sec)$

C_{Dt} discharge coefficient (eq. (B5)), dimensionless

D diameter inside vortex chamber where flow is Mach 1, m

D_o diameter of outlet orifice, cm

K_1 constant term (eq. (B16)), N/cm^2

K_2 constant term (eq. (B16)), dimensionless

k ratio of specific heats, dimensionless

$\dot{m}_i$ theoretical (ideal) flow through tangential nozzles (eqs. (B7) and (B12)), kg/sec

$\dot{m}_n$ normalizing term (eqs. (B2), (B9), and (B13)), kg/sec

$\dot{m}_o$ outlet mass flow, kg/sec

$\dot{m}_*$ normalized outlet mass flow (eq. (B2)), dimensionless

$\dot{m}_{*t}$ normalized outlet mass flow at cutoff point (eq. (B5)), dimensionless

P_e exhaust pressure, N/cm^2 abs

P_r radial supply pressure, N/cm^2 abs

P_{rt} radial supply pressure at cutoff point, N/cm^2 abs

P_t tangential nozzle supply pressure, N/cm^2 abs

P_* normalized pressure (eq. (B1)), dimensionless

P_{*t} normalized pressure at cutoff point, dimensionless

R_N Reynolds number, dimensionless

T_t temperature of gas upstream of tangential nozzles, K

V fluid velocity at Mach 1, m/sec

X radial inlet offset (fig. 5), mm

Y outer wall offset (fig. 5), mm

μ dynamic viscosity where flow is Mach 1, (kg)/(m)(sec)

ρ fluid density where flow is Mach 1, kg/m^3

Subscripts:

1 full-size valve

2 one-sixth-scale model valve

REFERENCES

1. Sanders, Bobby W.; and Mitchell, Glenn A.: Increasing the Stable Operating Range of a Mach 2.5 Inlet. Paper 70-686, AIAA, June, 1970.

2. Moorehead, J. R.: Development of the Boeing SST Inlet, Control, and Power System. Paper 670318, SAE, Apr., 1967.

3. Bauer, A. B.: Vortex Valve Operation in a Vacuum Environment. Paper 68-FE-47, ASME, May 1968.

4. Greber, Isaac; Koerper, P. E.; and Taft, C. K.: Fluid Vortex Amplifier Optimization. Proceedings of the Fluid Amplification Symposium, Vol. II, Harry Diamond Lab., Washington, D.C., Oct. 26-28, 1965, pp. 223-243. (Available as AD-623456.)

5. Roschke, E. J.; Pivirotto, T. J.: Similarity in Confined Vortex Flows. Rep. TR-32-789, Jet Propulsion Lab., California Inst. Tech. (NASA CR-67210), Aug. 15, 1965.

6. Mayer, E. A.; and Taplin, L. B.: Vortex Devices. Fluidics. E. F. Humphrey and D. H. Tarumoto, eds., Fluid Amplifier Associates, Inc., 1965, pp. 185-200.

7. Mayer, Endre A.: Large-Signal Vortex Valve Analysis. Advances in Fluidics. F. T. Brown, ed., ASME, 1967, pp. 233-250.

8. Larson, Ralph H.: Vortex Amplifier Parameters. Instr. Control Syst., vol. 39, no. 10, Oct. 1966, pp. 105-110.

9. Shapiro, Ascher H.: The Dynamics and Thermodynamics of Compressible Fluid Flow. Vol. 1. Ronald Press Co., 1953.

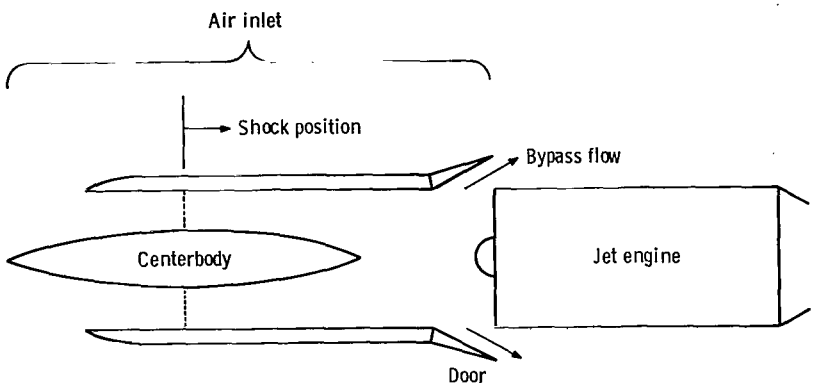

Figure 1. - Schematic illustration of supersonic jet-engine inlet.

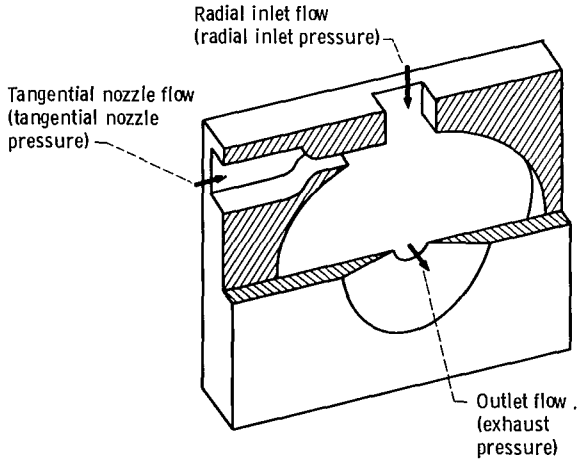

Figure 2. - Schematic illustration of the vortex valve.

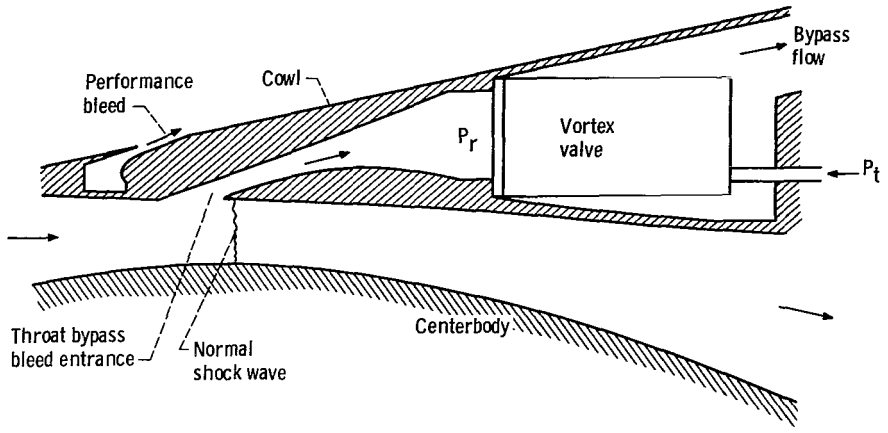

Figure 3. - Sketch of cowl showing forward-facing slot and vortex valve. Normal shock is shown in its proper position.

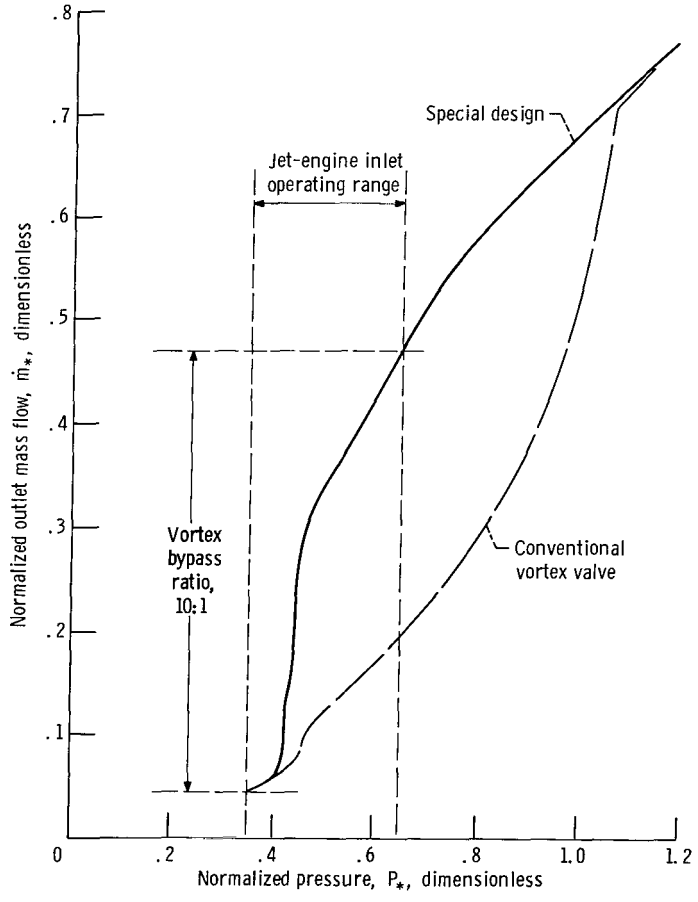

Figure 4. - General comparison between the valve described in this report and a conventional vortex valve. Data obtained from one-sixth-scale model.

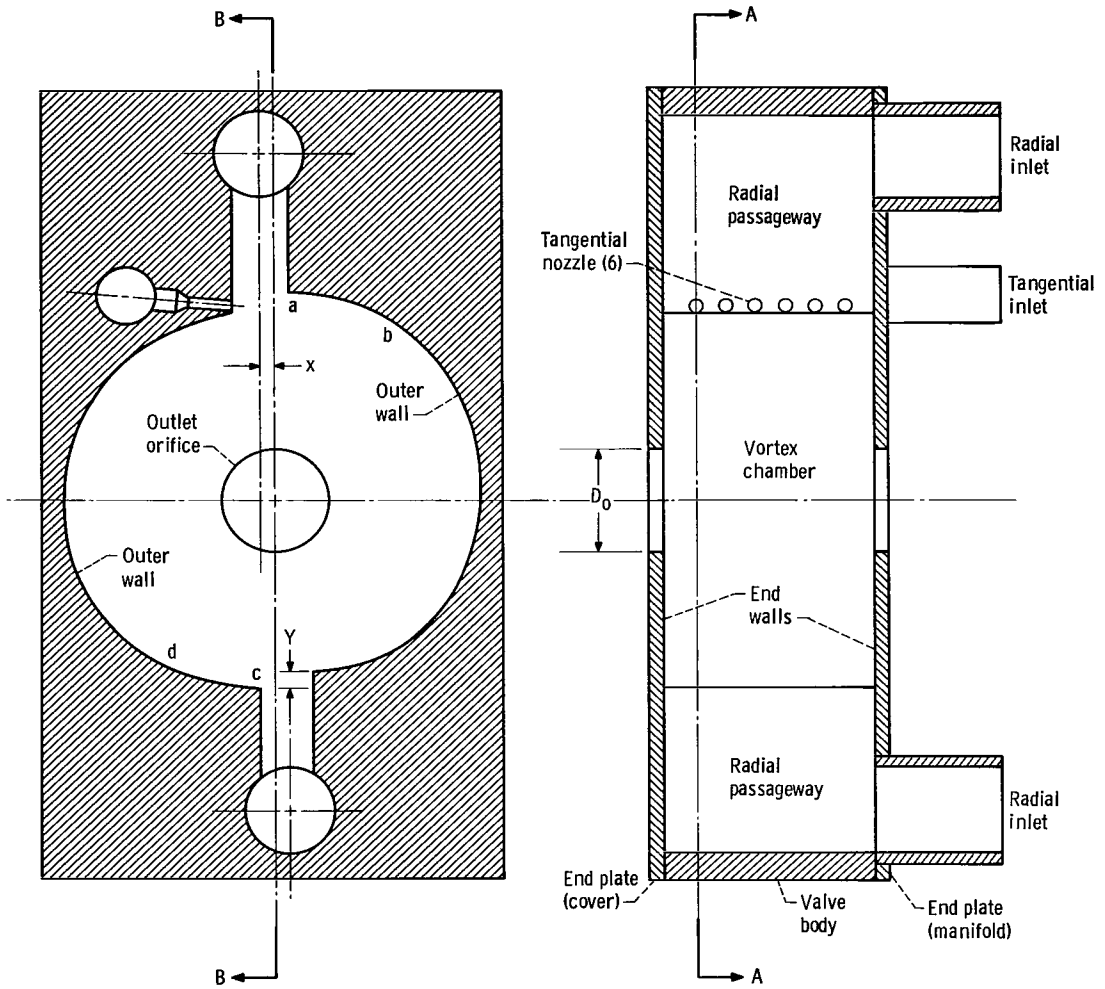

Figure 5. - Section views of vortex valve designed for stabilizing engine inlets.

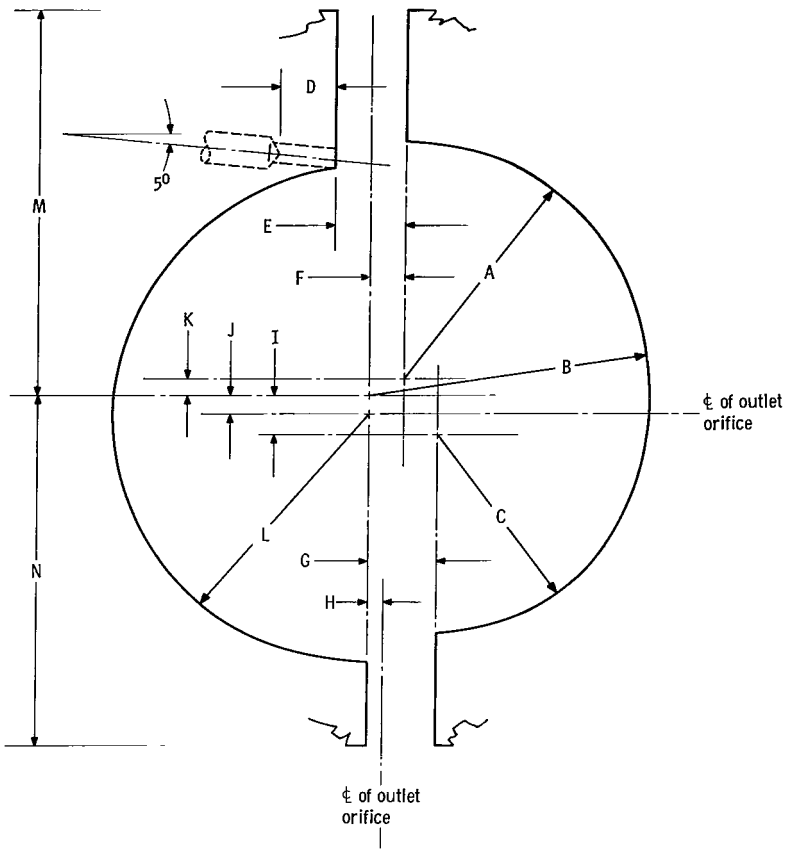

D_o = diameter of outlet orifice

A = B - F sec 30^0 = 1.8587 D_o	H = 0.1333 D_o
B = 2.1667 D_o	I = G tan 30^0 = 0.3079 D_o
C = B - G sec 30^0 = 1.5508 D_o	J = 0.1333 D_o
D = 0.416 D_o	K = F tan 30^0 = 0.1540 D_o
E = 0.553 D_o	L = 1.933 D_o
F = 0.2667 D_o	M = 3.00 D_o
G = 0.533 D_o	N = 2.75 D_o

Figure 6. - Profile of vortex chamber for valve models A, B, C, and D, and for final valve design.

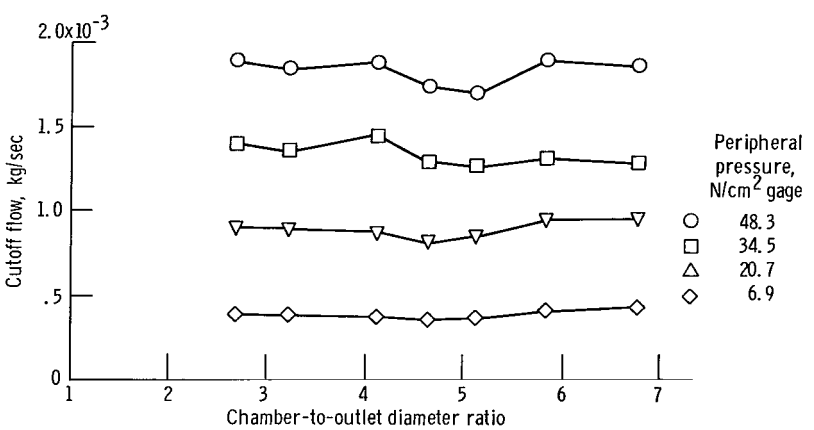

Figure 7. - Cutoff flow as affected by chamber diameter. Outlet orifice diameter, 3.22 millimeters; fluid, air at room temperature; outlet flow to atmosphere.

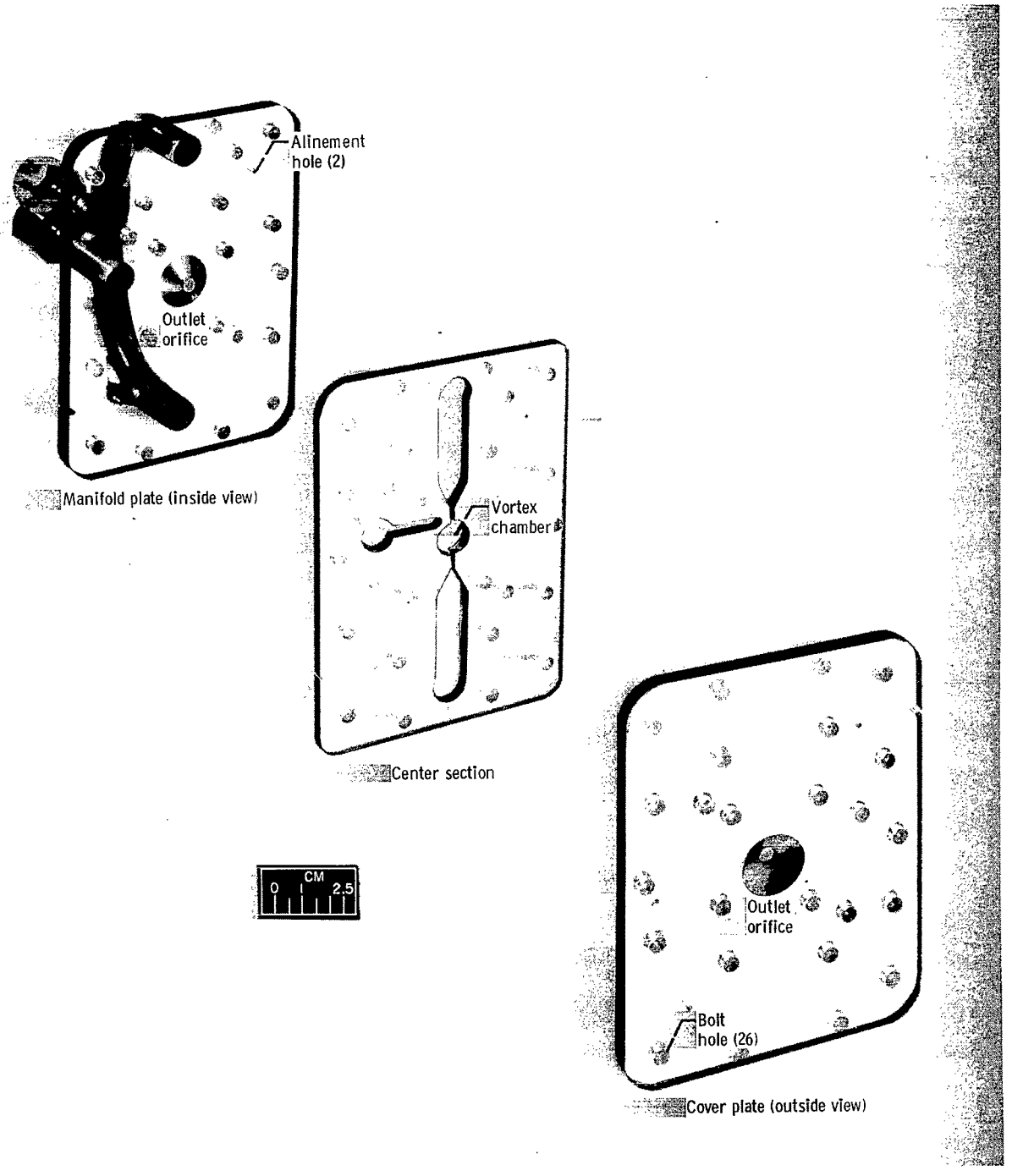

Figure 8. - Components of a one-sixth-scale test valve.

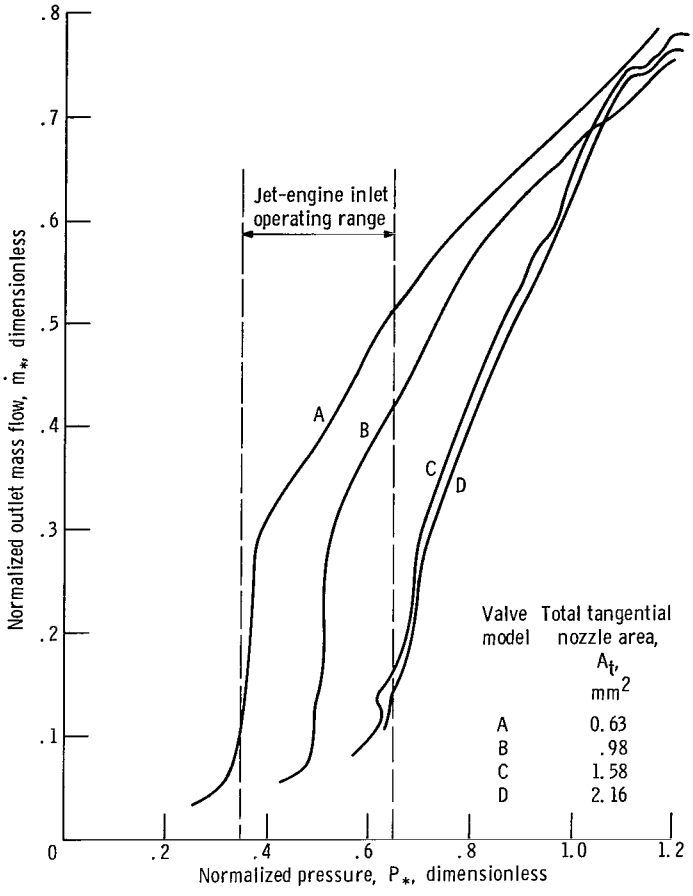

Figure 9. - Effects of tangential nozzle area on steady pressure-flow characteristics of model vortex valves.

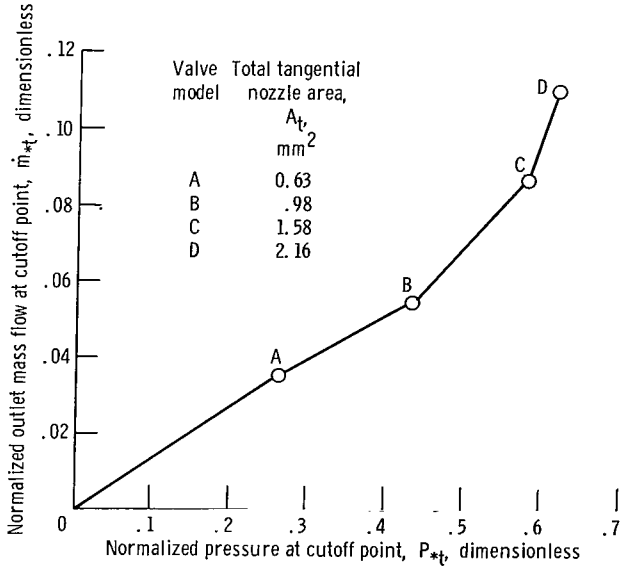

Figure 10. - Normalized pressure and flow at valve cutoff point for different tangential nozzle areas.

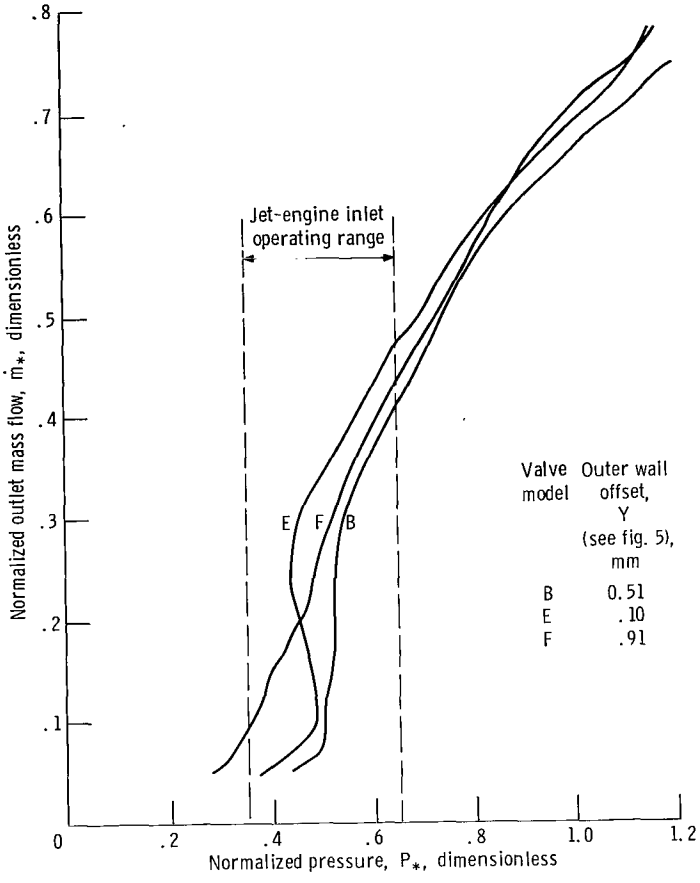

Figure 11. - Effects of wall offset on steady pressure-flow characteristics.

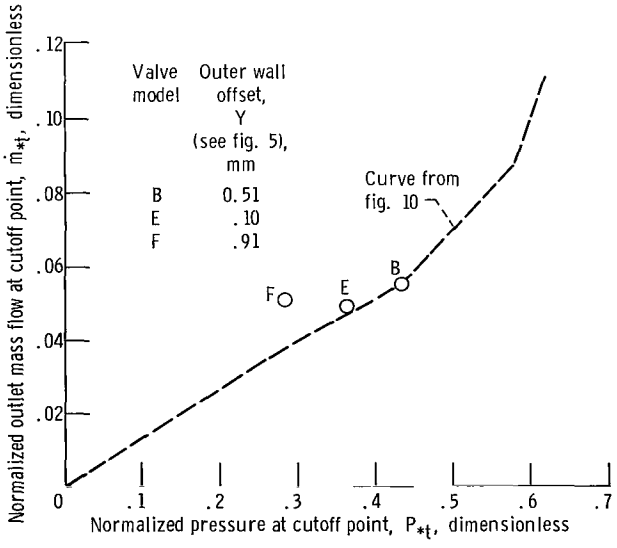

Figure 12. - Normalized pressure and flow at valve cutoff point for different wall offsets.

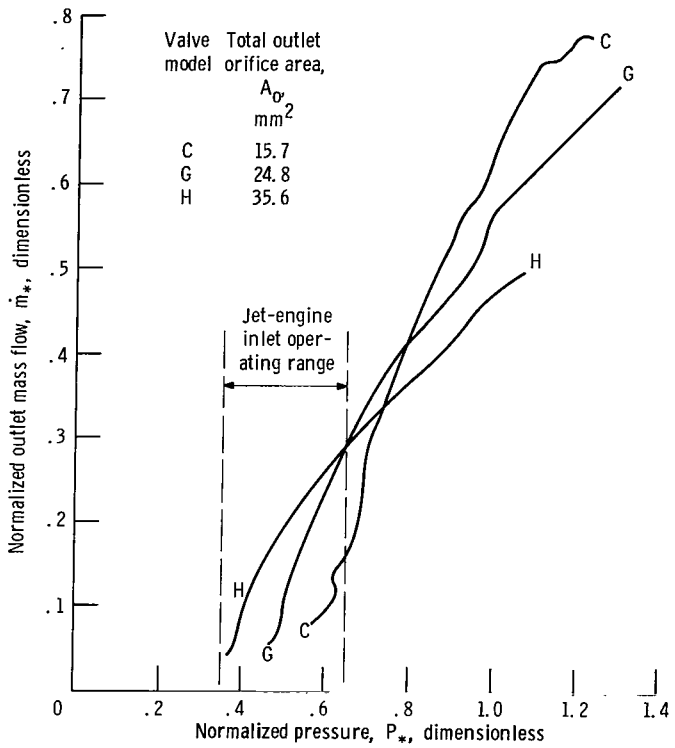

Figure 13. - Effects of outlet orifice area on steady pressure-flow characteristics.

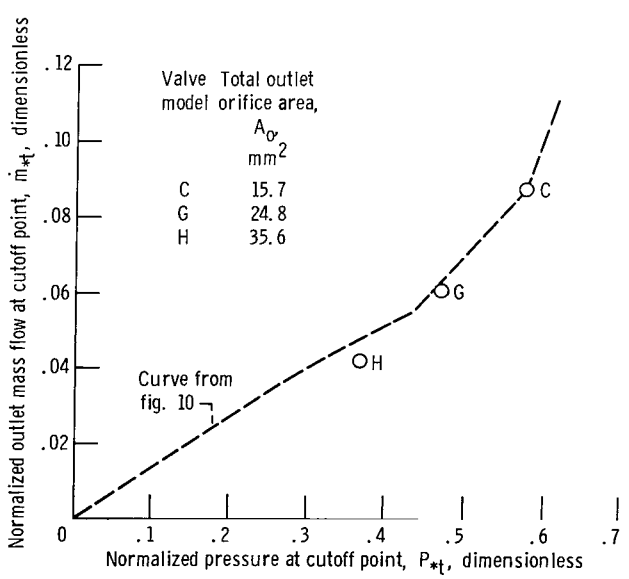

Figure 14. - Normalized pressure and flow at valve cutoff point for different outlet orifice areas.

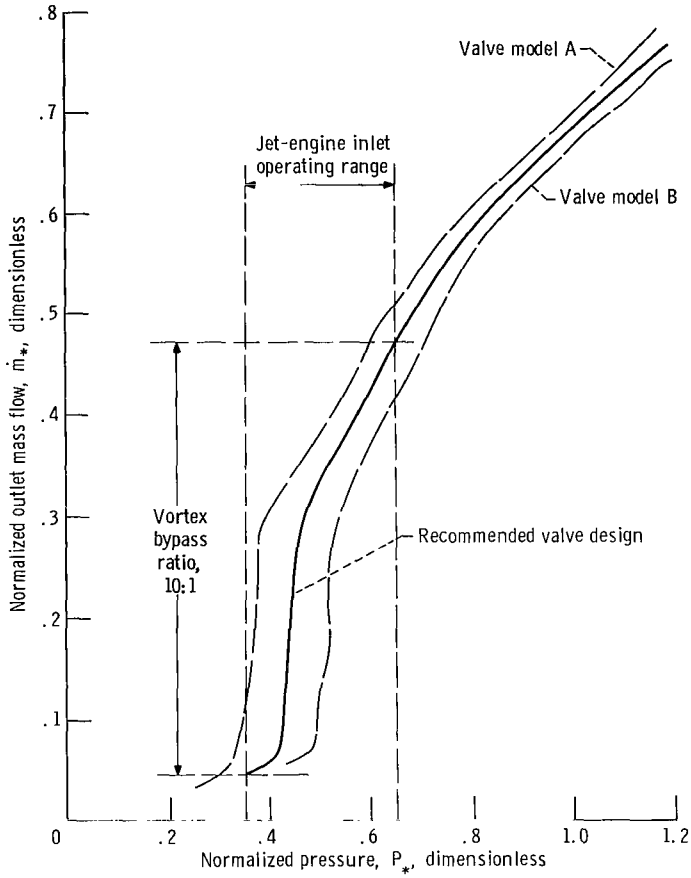

Figure 15. - Steady pressure-flow characteristics of recommended vortex valve design for experimental jet-engine inlet.

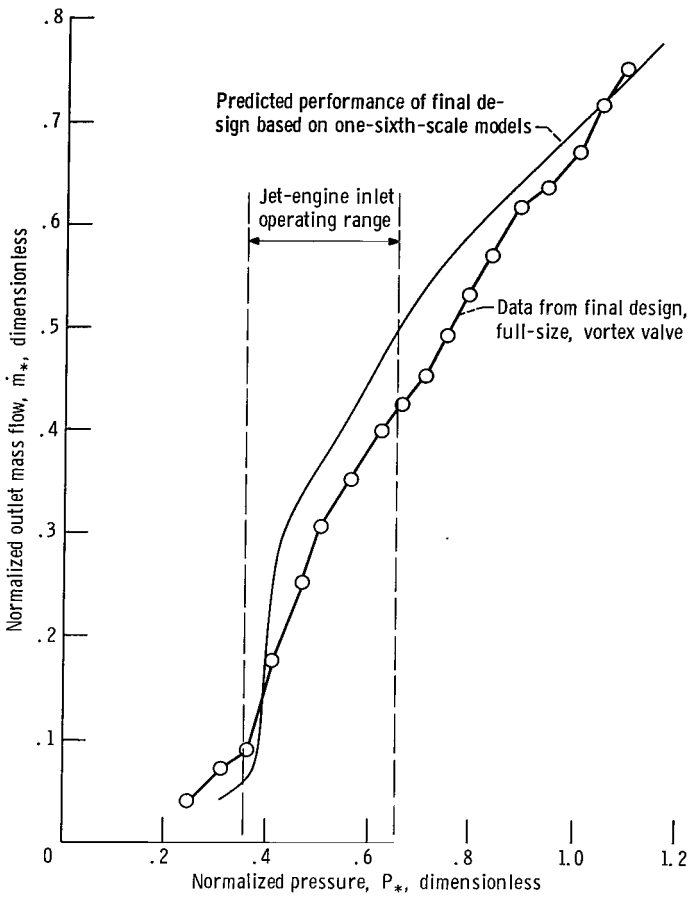

Figure 16. - Performance of full-size, final valve design. Tangential nozzle supply pressure, P_t, 8.1 N/cm^2 abs; exhaust pressure, P_e, 0.77 to 1.01 N/cm^2 abs; radial supply pressure, P_r, variable.

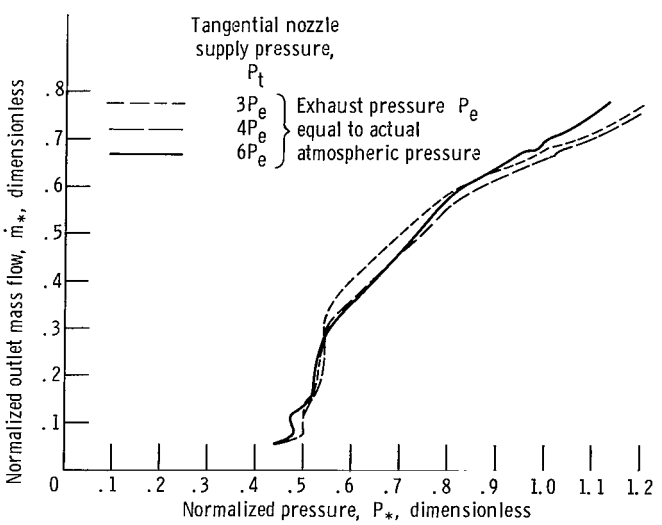

Figure 17. - Valve model B tested with variable radial supply pressure at three values of tangential nozzle supply pressure.

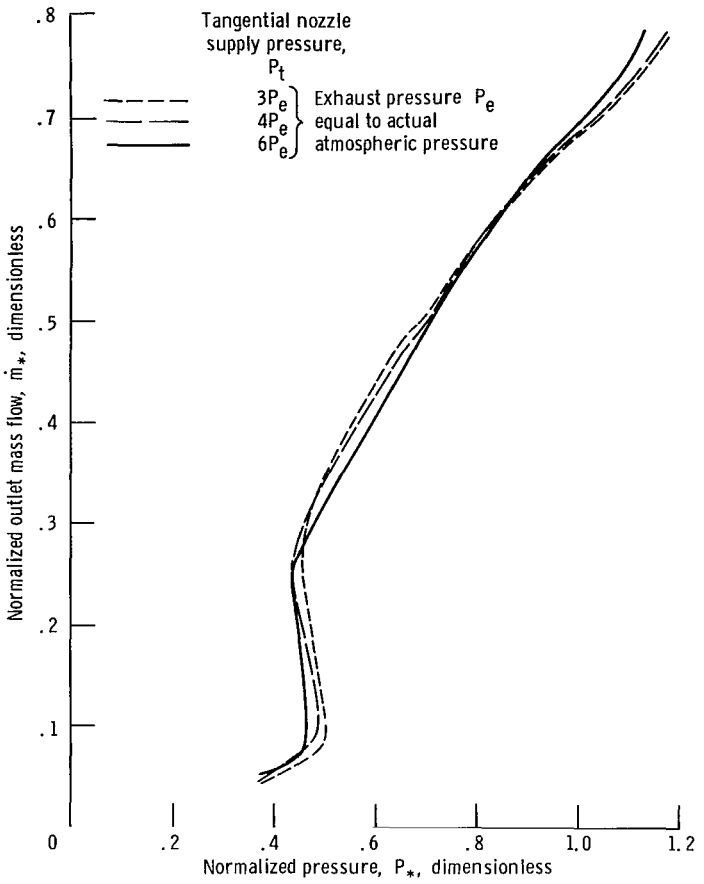

Figure 18. - Valve model E tested with variable radial supply pressure at three values of tangential nozzle supply pressure.

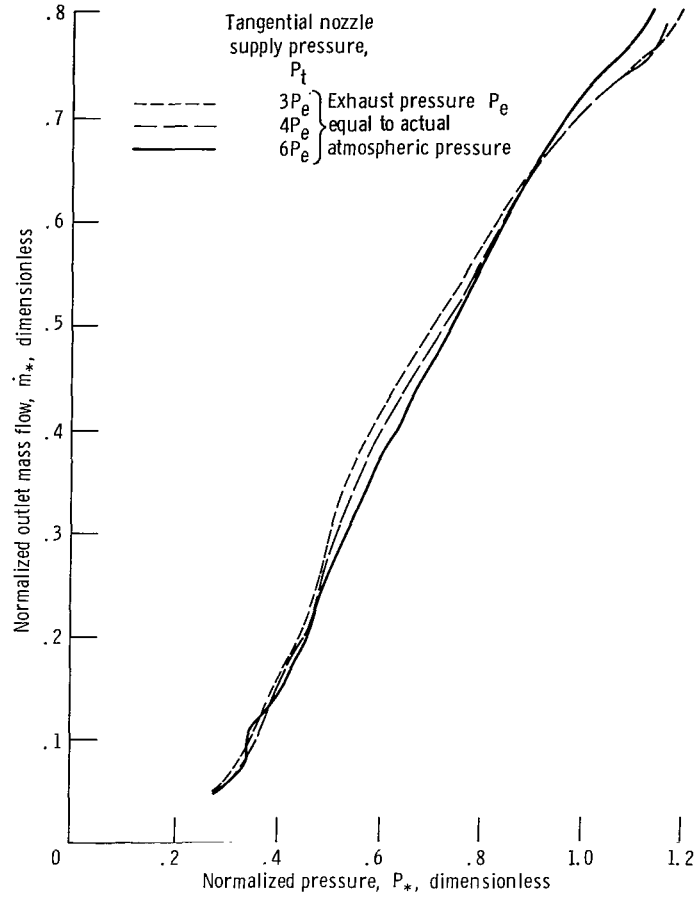

Figure 19. - Valve model F tested with variable radial supply pressure at three values of tangential nozzle supply pressure.

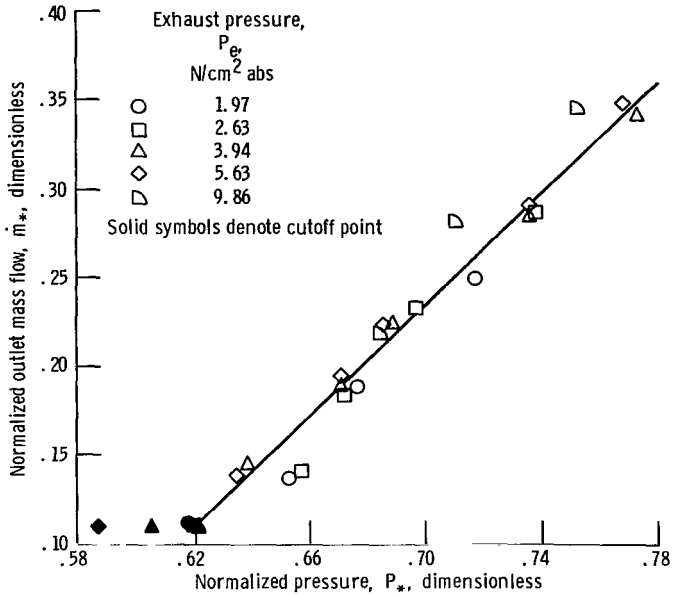

Figure 20. - Valve model D tested with variable radial supply pressure at five values of exhaust pressure. Tangential nozzle supply pressure, 39.4 N/cm^2 abs.

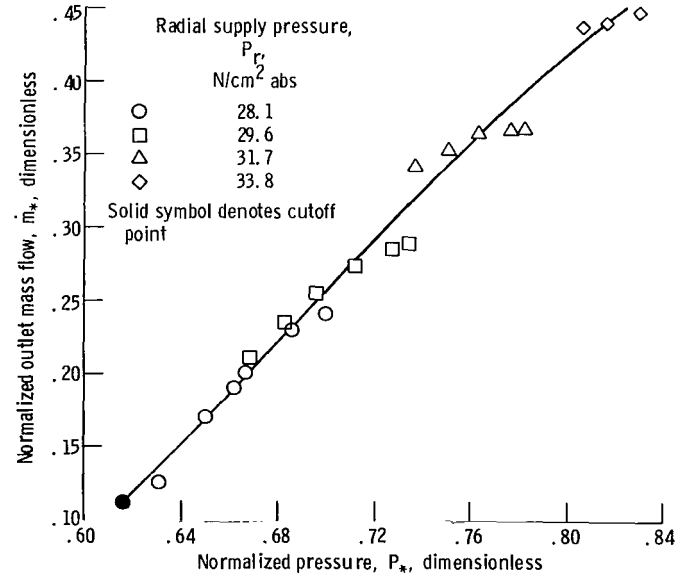

Figure 21. - Valve model D tested with variable exhaust pressure at four values of radial supply pressure. Tangential nozzle supply pressure, 39.4 N/cm^2 abs.

"The aeronautical and space activities of the United States shall be conducted so as to contribute . . . to the expansion of human knowledge of phenomena in the atmosphere and space. The Administration shall provide for the widest practicable and appropriate dissemination of information concerning its activities and the results thereof."

—NATIONAL AERONAUTICS AND SPACE ACT OF 1958

NASA SCIENTIFIC AND TECHNICAL PUBLICATIONS

TECHNICAL REPORTS: Scientific and technical information considered important, complete, and a lasting contribution to existing knowledge.

TECHNICAL NOTES: Information less broad in scope but nevertheless of importance as a contribution to existing knowledge.

TECHNICAL MEMORANDUMS: Information receiving limited distribution because of preliminary data, security classification, or other reasons.

CONTRACTOR REPORTS: Scientific and technical information generated under a NASA contract or grant and considered an important contribution to existing knowledge.

TECHNICAL TRANSLATIONS: Information published in a foreign language considered to merit NASA distribution in English.

SPECIAL PUBLICATIONS: Information derived from or of value to NASA activities. Publications include conference proceedings, monographs, data compilations, handbooks, sourcebooks, and special bibliographies.

TECHNOLOGY UTILIZATION PUBLICATIONS: Information on technology used by NASA that may be of particular interest in commercial and other non-aerospace applications. Publications include Tech Briefs, Technology Utilization Reports and Technology Surveys.

Details on the availability of these publications may be obtained from:

SCIENTIFIC AND TECHNICAL INFORMATION OFFICE

NATIONAL AERONAUTICS AND SPACE ADMINISTRATION

Washington, D.C. 20546